In vivo time-lapse microscopy reveals no loss of murine myonuclei during weeks of muscle atrophy

Jo C. Bruusgaard and Kristian Gundersen

Department of Molecular Biosciences, University of Oslo, Oslo, Norway.

Numerous studies have suggested that muscle atrophy is accompanied by apoptotic loss of myonuclei and therefore recovery would require replenishment by muscle stem cells. We used in vivo time-lapse microscopy to observe the loss and replenishment of myonuclei in murine muscle fibers following induced muscle atrophy. To our surprise, imaging of single fibers for up to 28 days did not support the concept of nuclear loss during atrophy. Muscles were inactivated by denervation, nerve impulse block, or mechanical unloading. Nuclei were stained in vivo either acutely by intracellular injection of fluorescent oligonucleotides or in time-lapse studies after transfection with a plasmid encoding GFP with a nuclear localization signal. We observed no loss of myonuclei in fast- or slow-twitch muscle fibers despite a greater than 50% reduction in fiber cross-sectional area. TUNEL labeling of fragmented DNA on histological sections revealed high levels of apoptotic nuclei in inactive muscles. However, when costained for laminin and dystrophin, virtually none of the TUNEL-positive nuclei could be classified as myonuclei; apoptosis was confined to stromal and satellite cells. We conclude that disuse atrophy is not a degenerative process, but is rather a change in the balance between protein synthesis and proteolysis in a permanent cell syncytium.

Introduction

Muscle atrophy and weakness is a major health problem related to inactivity, injury, disease, aging, and medication, and regaining muscle strength is an important factor for life expectancy and quality. The most important factor in maintaining or regaining muscle force is nerve-evoked contractile activity (1), and there is so far no remedy for inactivity-related atrophy other than by restoring or increasing physical activity (2). Thus, there is an interest in determining the fundamental biological mechanisms related to disuse atrophy in muscle.

The current literature suggests 2 major mechanisms for atrophy: first, proteolysis seems to be increased, mainly through activation of the ubiquitin-proteasome pathway (reviewed in refs. 2, 3). Secondly, protein synthesis is reduced (reviewed in ref. 4), and this has been related to a loss of myonuclei (5–17) by apoptosis (6, 8, 9, 12, 15, 18–27). Such mechanisms have been connected to neuromuscular disorders, in particular denervating disorders (reviewed in ref. 28), as well as to several experimental atrophy models including denervation (9, 16–24), nerve inactivation without Wallerian nerve degeneration (11, 12), and mechanical muscle unloading (6–8, 10, 25–27). A loss of nuclei during atrophy would imply that recovery of strength requires replenishment of nuclei from satellite cells, the muscle stem cells, and that potential intervention therapy would involve activation or substitution of such cells or interference with apoptotic pathways.

We set out to use what we believe to be a novel in vivo time-lapse imaging technique to directly observe the loss and replenishment of individual myonuclei in the intact animal. To our surprise, direct observation revealed that there is no loss of myonuclei during disuse atrophy. Apoptotic nuclei were abundant within the atrophying muscle tissue but confined to satellite and stromal cells.

Results

Time-lapse study of nuclei in denervated muscle demonstrated a constant number of myonuclei. An expression vector for GFP with a nuclear localization signal (nuclear EGFP [nucEGFP]) was either introduced by intracellular injection in vivo (29) or by electroporation (30). The stable expression of this vector allowed in situ time-lapse observations of nuclei confined within a single sarcolemma (Figure 1A). Unambiguous identification of each fiber at different time points was possible because each endplate has a unique fingerprint-shaped structure that is conserved over time (31). The synapse also served as a landmark that enabled us to find the same segment after several days or even weeks. In total, we reconstructed fiber segments from 30 fibers from 12 different animals. These segments had on average 55 ± 1.6 nuclei/mm fiber, a finding that is largely in agreement with publications counting isolated fixed muscle fibers stained with DAPI or hematoxylin (32, 33) or numbers calculated from cryosections (our own observations and, for example, refs. 16, 34).

Eleven fibers from 11 different animals were observed at multiple time points, and from these fibers 276 nuclei were followed for an average of 12 days during inactivity (Figure 1A). To ensure that identical segments were studied at the different time points, the segments were aligned by their endplates. None of the defined segments displayed changes of more than ±1 in the number of nuclei (Figure 1B), and these small changes could easily be attributed to slight variability in muscle stretch. On average, the fibers that were studied by time-lapse microscopy displayed 55% atrophy between the first and last time points of observation (Figure 1C).

Acute labeling of myonuclei in vivo revealed no loss of myonuclei during denervation atrophy. In order to study fibers without the presence of

Nonstandard abbreviations used: EDL, musculus extensor digitorum longus; nucEGFP, nuclear EGFP; TTX, tetrodotoxin.

Conflict of interest: The authors have declared that no conflict of interest exists.

Citation for this article: *J. Clin. Invest.* **118**:1450–1457 (2008). doi:10.1172/JCI34022.

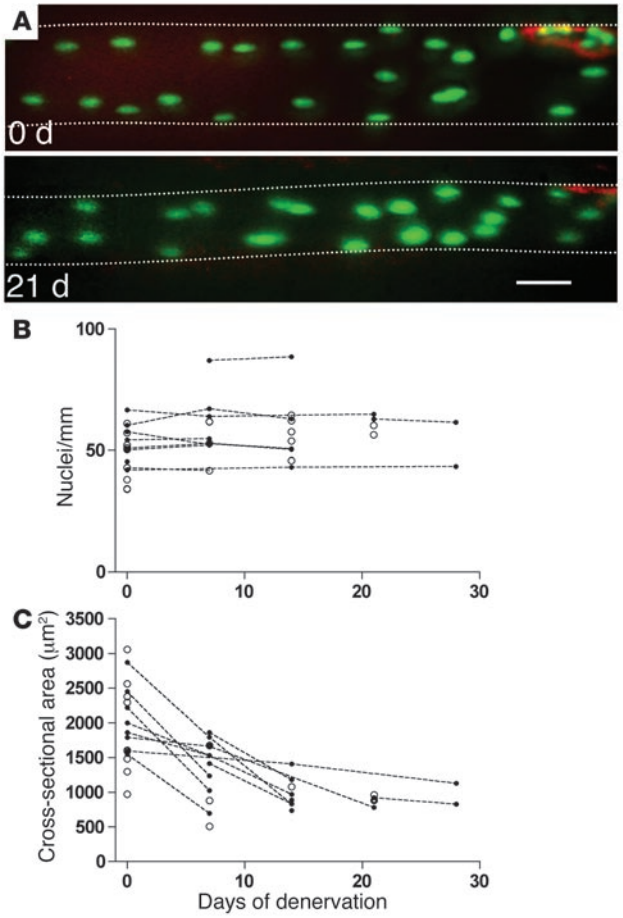

Figure 1
Time-lapse study of nuclei and atrophy in single muscle fibers in the EDL muscle after denervation. (**A**) Images of a representative muscle fiber after injection of an expression vector encoding nucEGFP (green) showing the same fiber observed at the time of denervation and again after 21 days. The neuromuscular endplate was stained by α-bungarotoxin (red). At both time points, 21 nuclei can be identified within the picture frame. Background staining of EGFP or fluorescent nucleotides in the cytosol made the fiber outline discernible, and an estimated cross-sectional area was calculated from the apparent diameter. The fiber boundaries are outlined for clarity. For the 2-dimensional illustrations presented in the figures, the image stacks were merged by the Project Z command in NIH ImageJ. Some out-of-focus information was removed from some of the planes, and different degrees of contrast enhancement were used in different parts of the final image to compensate for spatial differences in camera sensitivity and in staining intensity due to variable diffusion distances from the point of injection. Scale bar: 50 μm. (**B**) Summary of nuclei counts performed on picture stacks of fiber segments. Data representing multiple observations from the same fiber are indicated by filled symbols connected with broken lines. Single time-point observations of other fibers are indicated with open symbols. (**C**) For the same fibers as shown in **B**, cross-sectional area (CSA) was estimated by measuring the fiber diameter on micrographs.

foreign protein and without previous light exposure, we also studied muscle fibers by acute in vivo staining. Normal and denervated muscle fibers were acutely injected with fluorescent oligonucleotides at different time points after denervation. Like the nucEGFP labeling, this technique provides staining of the set of nuclei enveloped by a single sarcolemma, excluding satellite cells and stromal cells (35) (Figure 2A). By this staining method, 136 fibers from 15 different animals were studied. No differences in the number of nuclei were observed either in the fast, glycolytic musculus extensor digitorum longus (EDL) or the slow soleus muscle for up to 21 days after denervation (Figure 2B). During this time, the average estimated cross-sectional area of the injected fibers calculated from measurements of the fiber diameter observed through the microscope, was reduced by 51% and 55% in EDL and soleus, respectively (Figure 2C). This was similar to the 54% and 58% atrophy observed in other parts of these muscles when the whole muscle was studied on cryosections postmortem (Figure 2D). Thus, the acute in vivo imaging, confirming the findings obtained by time-lapse microscopy, showed that there was no loss of nuclei after denervation. Moreover, the acute approach excluded the possibility that the constant nuclear number is related to the presence of foreign protein or repeated imaging.

There is no loss of myonuclei during nerve block–induced atrophy. Denervation is perhaps the most dramatic form of atrophic stimuli. Although different forms of disuse conditions probably trigger similar response mechanisms, products of nerve degeneration and inflammation might in themselves have effects on the muscle (1, 36). We therefore used an alternative approach to induce muscle atrophy, i.e., blocking nerve activity by blocking the voltage-gated sodium channels by tetrodotoxin (TTX). In the EDL, 47 fibers from 7 animals were injected with fluorescent oligonucleotides and studied as described above. Consistent with results obtained from denervation studies, we observed no loss of myonuclei (Figure 3, A and B) despite an average atrophy of 35% in the injected fibers after 21 days of nerve block (Figure 3C). We concluded that there is no loss of nuclei after disuse even when the nerve is intact.

There is no loss of myonuclei after atrophy caused by unloading. Some of the literature connecting atrophy and loss of myonuclei has been based on experiments in which the muscles have been unloaded, but with an intact nerve supply (6–8, 10, 25–27). We unloaded the EDL muscle by tenotomizing the antagonist muscles (see Methods), which led to 18% atrophy (Figure 4). This was similar to results obtained for unloading with hindlimb suspension for comparable time periods in the same muscle in rats (10). In contrast to previous studies, however, we observed no significant loss of myonuclei (Figure 4).

Thus, 3 different methods for inducing atrophy essentially led to the same conclusion: that atrophy was not accompanied by loss of nuclei.

Apoptosis in inactive muscles is restricted to stromal and satellite cells. Since we found no loss of myonuclei during atrophy, we went on to reinvestigate whether we could detect apoptosis in atrophying muscles. When normal muscles were subjected to TUNEL staining, very little apoptosis was observed. Of the approximately 16,000 nuclei we screened in 20 sections from 9 different EDL and soleus muscles, we found only 9 apoptotic nuclei, on average about 0.5 per section. In contrast, during the first days after denervation, the number of apoptotic nuclei increased sharply (Figure 5), and after 21 days, 20 ± 5.3 and 46.5 ± 7.0 TUNEL-positive nuclei per section were detected in EDL and soleus muscles, respectively. Also, TTX-blocked muscles showed increased apoptosis but significantly less than that observed after denervation — 10 ± 1.4 nuclei per section after 21 days of inactivity (Figure 5B). These findings are in agreement with previous studies on denervation and other forms of disuse atrophy (6, 8, 9, 19, 24).

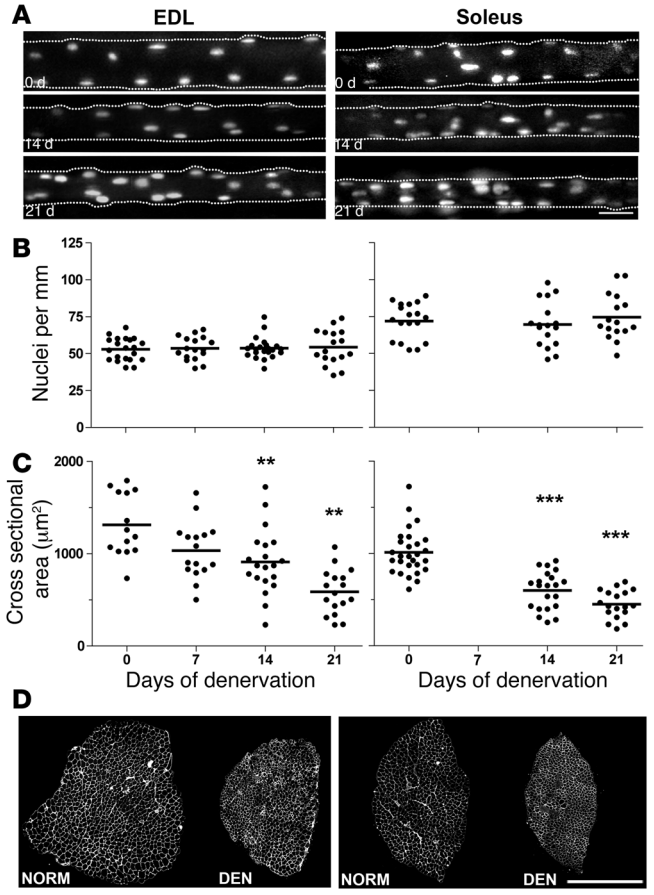

Figure 2
The effect of denervation on nuclei number and atrophy of single muscle fibers studied by acute in vivo staining and imaging in live animals. Fluorescent oligonucleotides were injected into single fibers in the EDL (left panels) and soleus (right panels) muscles at 0–21 days after denervation. (**A**) Images of representative single muscle fibers. See legend of Figure 1 for details about image processing for the 2-dimensional illustrations. Scale bar: 25 μm. The number of nuclei (**B**) and the cross-sectional area (**C**) were calculated from the image stacks. Horizontal lines indicate means; asterisks indicate statistical differences from normal values (**$P < 0.01$; ***$P < 0.001$). (**D**) The degree of atrophy after 21 days of denervation is illustrated by laminin-stained cryosections in. Scale bar: 500 μm.

Apoptosis in muscle tissue does not, however, necessarily reflect myonuclear apoptosis, as there are 3 main populations of nuclei in muscle: (a) nuclei belonging to stromal cells, (b) nuclei belonging to muscle satellite cells, situated within the basal lamina of muscle fibers, and (c) the myonuclei proper, which are situated inside the sarcolemma. The latter constitute approximately half of the nuclei in the tissue.

In order to identify the myonuclei proper, sections labeled with TUNEL and Hoechst dye 33342 were immunostained with dystrophin, a muscle cytoskeleton protein that visualizes the muscle fiber cortex (37, 38) (Figure 6, A–C). We interpreted nuclei with its mass center outside the dystrophin "ring" to either belong to satellite or stromal cells (Figure 6, A and B), and such nuclei frequently were TUNEL positive (Figure 6A). Similarly, we considered nuclei that had their mass center inside the dystrophin ring to be myonuclei. Figure 6, A and B, shows numerous examples of such myonuclei, but of the approximately 27,000 myonuclei that were screened 3–21 days after denervation, only 4 (2 in EDL and 2 in soleus) were TUNEL positive (0.015%, Figure 6D). One of these is illustrated in Figure 6, B and C. The additional finding that none of the 5,500 myonuclei screened on sections from the 3 TTX-blocked muscles was TUNEL positive confirmed that apoptosis of myonuclei is extremely rare after inactivity.

The finding that virtually none of the myonuclei were apoptotic allowed us to selectively study apoptotic satellite cells by laminin staining labeling the basal lamina. We considered nuclei with mass centers within the laminin ring to be myonuclei or belong to satellite cells, and based on the findings above, virtually all the TUNEL-positive cells in this category would be satellite cells (Figure 7A). The number of positive cells within the laminin ring increased sharply after denervation (Figure 7B).

Nuclei with mass centers outside the laminin ring were defined as stromal cell nuclei (Figure 7C). Denervation also led to a sharp increase in the TUNEL-positive fraction of this group of nuclei (Figure 7D). At 21 days, 2% and 6% of the stromal cells were TUNEL positive in EDL and soleus, respectively. In the muscles that had been blocked with TTX, 1% of the stromal cells were TUNEL positive. We conclude that disuse induces apoptosis both in satellite cells and stromal cells.

Lastly, we counted the number of myonuclei on sections stained for dystrophin. These data essentially confirmed the data obtained by in vivo imaging: the number of myonuclei and muscle fibers was essentially unaltered in the denervated muscles, in spite of significant atrophy (Figure 8).

Discussion

Our data indicate that disuse muscle atrophy is not accompanied by loss of nuclei. Thus, atrophy is not a degenerative process, but rather is simply a change in the balance between protein synthesis (4) and proteolysis (2, 3) in the permanent cell syncytia. Consequently, intervention efforts should focus on intracellular regulatory mechanisms related to protein degradation (2, 3) or synthesis (see ref. 39) and not on regeneration from stem cells.

Skeletal muscle cells are one of few syncytia in mammals and one of the cell types that show the greatest ability to change size under different physiological and pathological conditions. In muscle and other syncytia there has been a classical concept that there is a constant "karyoplasmatic" ratio (see, for example, ref. 40), and hereto it has been widely accepted that muscle cell size is closely correlated to the number of myonuclei (for recent reviews, see refs. 41–43, but see also ref. 44). Our results suggest that the simple karyoplasmatic model with constant myonuclear domain volumes might have to be revised, at least with respect to atrophy.

Disuse does, however, induce apoptotic activity in muscle stromal and satellite cells. Although previous authors have suggested that some apoptotic nuclei observed in denervated and other disused muscles are myonuclei (6, 8, 9, 19, 24), the identification of the nuclei has not been unambiguous. There are several methodological uncertainties involved in the preparation and the subsequent light microscopic evaluation of cryosections, such as tissue distortion and displacement of organelles. In particular, the close proximity of satellite cells to muscle fibers makes it difficult to distinguish between nuclei belonging to satellite cells and muscle fibers at the light microscopy level.

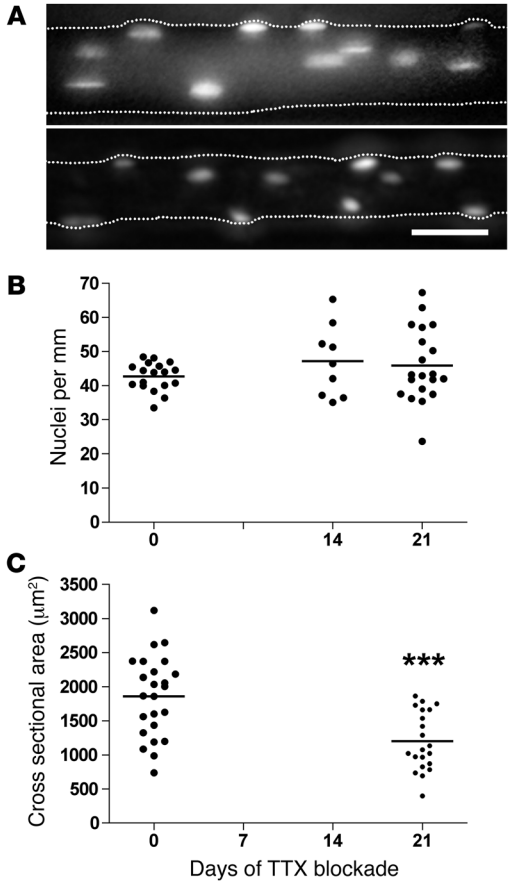

Figure 3
The effect of blocking nerve-evoked impulse activity on nuclei number and atrophy of single muscle fibers studied by acute in vivo staining and imaging in live animals. Fluorescent oligonucleotides were injected into single muscle fibers in EDL muscles at 0–21 days after starting a TTX block. (**A**) Representative images of single fibers. See legend of Figure 1 for details about image processing for the 2-dimensional illustrations. The number of nuclei (**B**) and the cross-sectional area (**C**) were calculated from image stacks. Horizontal lines indicate means; asterisks indicate statistical differences from normal values (***$P < 0.001$); scale bar: 25 μm.

Given the methodological uncertainties, we do not regard our observation of 4 apoptotic myonuclei out of approximately 27,000 (0.015%) as evidence for myonuclear apoptosis. On the other hand, in evaluating TUNEL staining, one should keep in mind that the time window within which a given nucleus might be identified could be as short as 2 hours (45). Thus, in apoptotic tissue, at any given time point, few nuclei undergoing apoptosis might be in the right apoptotic stage for it to be labeled with TUNEL. If accepting the 4 apoptotic myonuclei as bona fide, however, the frequency of 0.015% would imply that, even accumulated over a period of 21 days, less than 4% of myonuclei would be lost due to apoptosis (see Methods for calculation details), far too few to be significant for the observed atrophy.

Due to technical limitations such as EGFP build-up and difficulties with injecting severely atrophied fibers, our data were limited to the first few weeks of inactivity. The rate of atrophy and the apoptotic activity are reported to be highest during this initial period (6, 18, 24), but our data do not exclude the possibility that myonuclear apoptosis might occur after longer disuse periods. A previous study on fixed and teased fibers suggested, however, that the number of associated nuclei might not be reduced for up to 4 months of denervation in mice (32). Although this technique did not distinguish between satellite cells and myonuclei, the finding opens up the possibility that there is no loss of myonuclei even after very long disuse periods. If nuclei and fiber integrity persist even in the extremely atrophic fibers induced by long-term disuse, this might explain the remarkable recovery of muscle strength when nerve activity is restored or substituted by electrodes even after prolonged inactivity both in rodents (46) and in humans (47).

Methods

Animal experiments. The animal experiments were approved by the Norwegian Animal Research Authority and were conducted in accordance with the Norwegian Animal Welfare Act of December 20, 1975. The Norwegian Animal Research Authority provided governance to ensure that facilities and experiments were in accordance with The Animal Welfare Act, National Regulations of January 15, 1996, and the European Convention for the Protection of Vertebrate Animals Used for Experimental or Other Scientific Purposes of March 18, 1986.

Female NMRI mice were used. All imaging and surgeries were performed under deep anesthesia induced by intraperitoneal injections of 5 μl per gram body weight of Equithesin (Ullevål Sykehus; 42.5 mg/ml chloral hydrate and 9.7 mg/ml pentobarbitone). Depth of anesthesia was checked

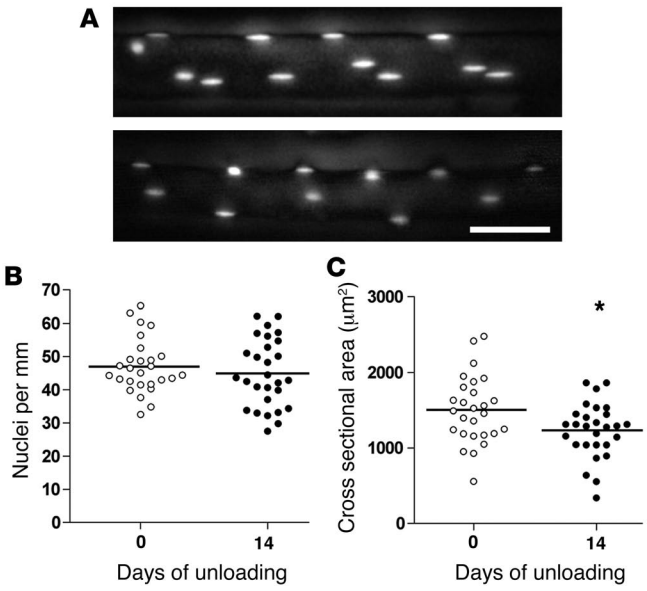

Figure 4
The effect of unloading on nuclei number and atrophy of single muscle fibers studied by acute in vivo staining and imaging in live animals. Fluorescent oligonucleotides were injected into single muscle fibers in EDL muscles at 0 and 14 days after unloading. (**A**) Representative images of single fibers. See legend of Figure 1 for details about image processing for the 2-dimensional illustrations. The number of nuclei (**B**) and the cross-sectional area (**C**) were calculated from image stacks. Horizontal lines indicate means; asterisk indicates statistical differences from normal values (*$P = 0.03$); scale bar: 25 μm.

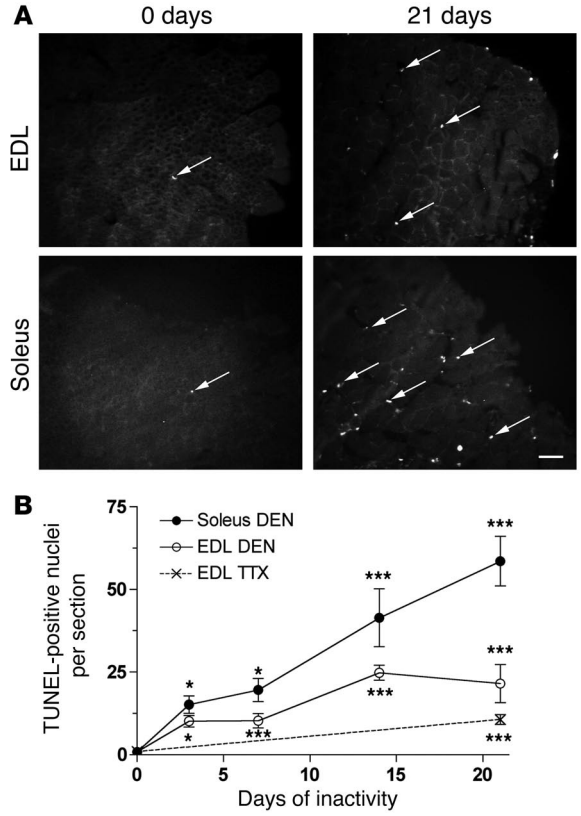

Figure 5
Apoptosis in normal and inactive muscles. (**A**) Representative images of TUNEL-stained cryosections from normal EDL and soleus muscles and 21 days after denervation of the muscles. Arrows indicate examples of apoptotic nuclei. (**B**) Counts (means ± SEM) from 6–10 sections from muscles that were denervated or TTX blocked for 0–21 days. Asterisks indicate statistical differences from normal values (*$P < 0.05$; ***$P < 0.01$). Scale bar: 25 μm.

regularly by pinching the metatarsus region of the limb, and additional doses of 1 μl/g were given if necessary.

Denervation was performed by surgically exposing the sciatic nerve in the thigh and then removing a 1-cm-long section of the nerve to prevent reinnervation.

The method for impulse block of the sciatic nerve with TTX has been described previously (48, 49). In brief, the TTX was delivered with a capillary implanted beneath the epineurium of the sciatic nerve. To ensure that the block was effective, the absence of the toe-spreading reflex and the withdrawal reflex were regularly checked and were taken together with the lack of use of the lower leg as parameters of a successful paralysis.

For unloading of the EDL muscle, the tendons and the most distal third of the antagonist muscles gastrocnemius, soleus, and plantaris were resected. In order to avoid complications related to regeneration and reattachment of the resected tendons, we limited the observation period to 14 days. The resected area was inspected after 14 days, and none of our animals displayed reattachment.

Labeling of nuclei for time-lapse microscopy. In order to label single fibers for prolonged periods of time, a plasmid, pEGFP-Nuc, was constructed, in which nucEGFP is driven by the CMV promoter. EGFP was cut out from pEGFP-C1 (Clontech) with NheI and BsrGI, and this fragment substituted the NheI-BsrGI fragment in pECFP-Nuc (Clontech). In half of the fibers reported here, this construct was injected intracellularly into single fibers as described previously (29). In brief, each fiber was penetrated once and a 1-μg/μl plasmid solution was injected over a few minutes via a micropipette using pressure pulses. We have previously shown that volumes of around 10 pl, less than 1% of the fiber volume, are typically injected during this procedure (29).

For the other half of the fibers, DNA was transfected by electroporation similar to what we have described before (30). For the present study, the muscle surface was bathed in a 1-μl/μg DNA solution, and subsequently 5 trains of 1,000 bipolar square pulses (10 V for 200 μs in each direction) were run across the muscle by 2 silver electrodes. It was important that only a few surface fibers were transfected in order to avoid confusing nuclei from adjacent fibers.

There were no differences in the results obtained by injection and electroporation, and mononuclear cells were never seen labeled after myofiber injection and were also exceedingly rare after electroporation.

For all nucEGFP experiments, an NMRI/TIE2-GFP hybrid mouse strain was used (50). The TIE2 strain is a transgenic line expressing EGFP in vascular tissue and was used to avoid immunological reactions to EGFP. In the heterozygous hybrids used in this study, EGFP from the transgene was not visually detectable in our system, so the transgene EGFP did not interfere with our observations. At high concentrations, however, nucEGFP

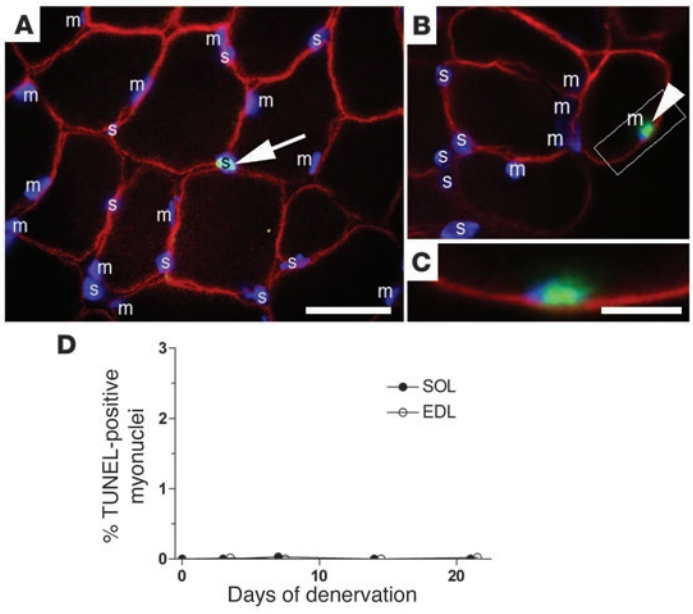

Figure 6
Apoptosis in nuclei identified as myonuclei was extremely rare. (**A**–**C**) Sections triple-stained with antibodies against dystrophin (red), TUNEL (green), and Hoechst dye 33342 (blue). Myonuclei (m) or nuclei that are either satellite or stromal cells (s) are indicated. A TUNEL-positive nucleus outside the dystrophin staining, i.e., a stromal or satellite cell, is indicated in **A** (arrow). Scale bar: 25 μm. One of the only 4 apoptotic nuclei in the present study that appeared to be a myonucleus is illustrated at the same magnification in **B** (arrowhead), with the framed area at higher magnification shown in **C** (scale bar: 10 μm). (**D**) Percentage of TUNEL-positive myonuclei after denervation. The symbols for EDL were shifted slightly sideways for clarity. Means ± SEM; $n = 6–10$ sections.

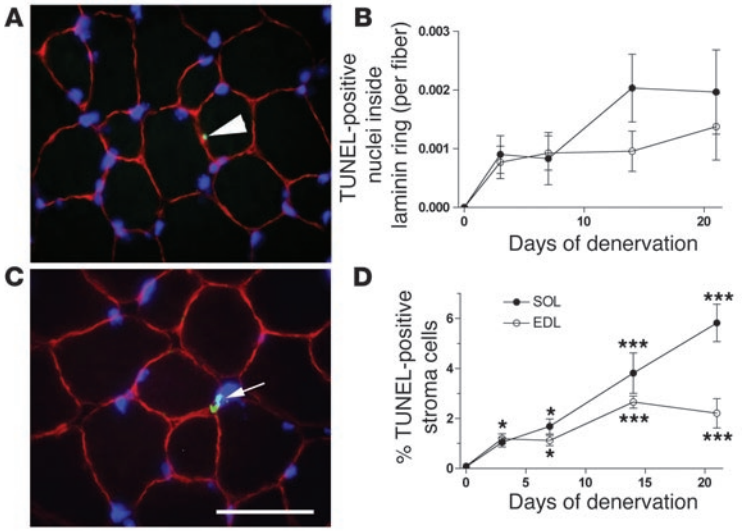

Figure 7
Apoptosis of satellite and stromal cells. Sections were triple stained with antibodies against laminin (red), TUNEL (green), and Hoechst dye 33342 (blue). TUNEL-stained nuclei inside the laminin ring were regarded as apoptotic satellite cells (arrow in **A**), since virtually no myonuclei were apoptotic (Figure 6). The number of such cells at various times after denervation is shown in **B**. Kruskal-Wallis test indicated that the increase after denervation was significant in both the EDL and the soleus, but since all sections in normal muscles and several sections from denervated muscles displayed 0-values for TUNEL-positive cells inside the laminin ring, post-testing for each time point was precluded. An example of a TUNEL-stained cell nucleus (arrow) outside the basal lamina indicative of an apoptotic stromal cell is shown in **C**, and the number of such cells at various times after denervation is shown in **D**. Asterisks indicate statistical differences from normal values (*$P < 0.05$; ***$P < 0.001$). Scale bar: 25 μm. Means ± SEM; n = 6–10 sections.

expression seemed to be cytotoxic even in these animals. Thus, some fibers expressing nucEGFP at high levels disappeared or showed signs of pathology, such as central nuclei, clustering of nuclei and swelling, selectively in regions with high nucEGFP expression. Even though other parts of the fiber with nucEGFP expression at lower levels looked normal, all fibers with abnormalities were excluded from further analysis.

Injection or electroporation of the plasmid was performed 1 week before the denervation or implantation of TTX capillaries, and the first observation (day 0) was made during this second operation.

Acute nuclear staining. For acute staining of nuclei in normal and denervated fibers not expressing a foreign protein, single soleus or EDL fibers were injected with 5′-Oregon Green–labeled phosphorothioated oligonucleotides (5.0×10^{-4} M; Biognostik) and 2 mg/ml of Cascade Blue dextran (Molecular Probes) in an injection buffer (10 mM NaCl, 10 mM Tris, pH 7.5, 0.1 mM EDTA, and 100 mM potassium gluconate), as described before (35). Satellite cells were not labeled since the oligonucleotides are water soluble and there are no gap junctions between satellite cells and the muscle fibers (see discussion in ref. 35).

In vivo imaging. In vivo imaging was pioneered by Lichtman and collaborators (31), with adaptations that we have described previously (29, 35). Fiber segments of 250–1,000 μm were analyzed by acquiring images in different focal planes 5 μm apart each on an Olympus BX-50WI compound microscope with a ×20, 0.9 NA water immersion objective. All images were taken with a SIT camera (Hamamatsu C2400-08) coupled to an image processor (Hamamatsu ARGUS-20). By importing the images to a Macintosh computer running Adobe Photoshop and NIH ImageJ software, a stack was generated and used to count all the nuclei in the segment. The counting of nuclei was performed by evaluating all the images in each stack.

The neuromuscular junction was visualized by applying the snake venom α-bungarotoxin conjugated with rhodamine (Molecular Probes) to the surface of the muscle for 2–3 min at a nonblocking concentration of 1 μg/ml (51).

Immunohistochemistry. Muscles were excised, embedded in OCT Tissue-Tek, frozen slightly stretched in melting isopentane, and stored at –80°C before being cryosectioned at 10 μm. DNA fragmentation associated with apoptosis was detected by TUNEL, using the TdT-FragEL detection kit according to the manufacturer's instructions (EMD Biosciences). The sections were then blocked with 1% BSA and costained either with anti-dystrophin (Sigma-Aldrich) or anti-laminin (Sigma-Aldrich) monoclonal antibodies at 1:200 dilution and 1:50 dilution, respectively. Nuclei were

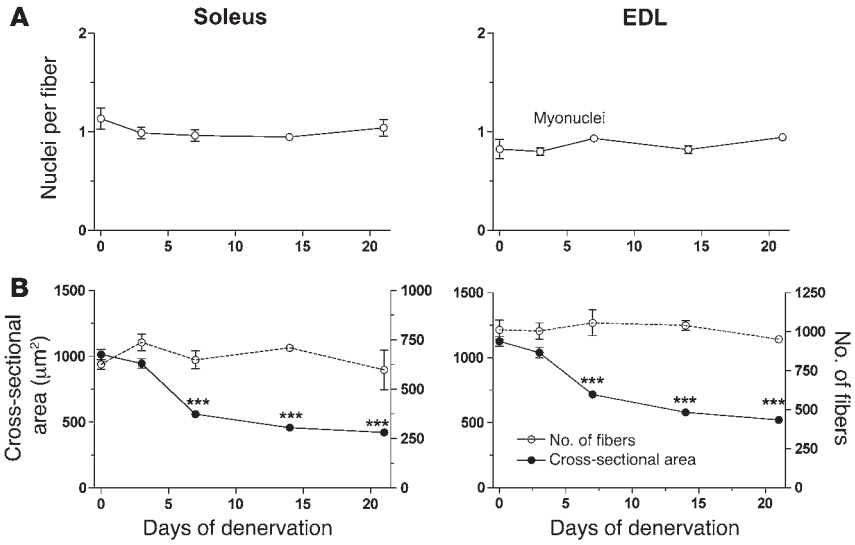

Figure 8
Quantification from cryosections stained for dystrophin of number of myonuclei (**A**), number of muscle fibers (**B**), and fiber cross-sectional area (**B**) after denervation. Means ± SEM of 5–6 muscles at each time point. ***$P < 0.001$.

costained using Hoechst dye 33342 at 5 μg/ml in PBS. Nuclei were counted as TUNEL positive only if colocalization of the Hoechst dye and TUNEL staining was observed. Slides were observed in an Olympus fluorescence microscope with a ×60 water immersion objective.

Turnover calculations of nuclei. Although cells might be committed to apoptosis for several hours, time-lapse microscopy has revealed that some of the morphological characteristics of apoptosis last only approximately 2 h (45). Thus, only a few cells undergoing apoptosis might be identifiable as such at any time point, and the quantitative significance of apoptosis for cell turnover may easily be underestimated. In order to evaluate the significance of the observed apoptotic frequencies (f), we calculated the fraction of nuclei undergoing apoptosis (F) over a certain time period (T) with the identification time window (t) by the formula $F = f \times T/t$. This formula assumes that all nuclei are subjected to a certain probability of entering apoptosis and that there is no significant net loss of nuclei (see Results).

Statistics. Effects of inactivity on populations of nuclei were tested by the nonparametric tests Mann-Whitney or Kruskal-Wallis with Dunn's post-hoc test for comparison of each time point with pre-inactivity values. $P < 0.05$ was considered significant. Data are given as mean ± SEM.

Acknowledgments

This work was supported by Norwegian Research Council grant no. 136134/V40 and European Commission grant no. QLK6-CT-2000-00530. We are grateful to Arild Njå and Eva Aaboen Hansen for help with the TTX experiments and to Shuo-Wang Qiao, Marit J. Bakke, and Ida G. Lunde for comments on the manuscript.

Received for publication September 22, 2007, and accepted in revised form January 9, 2008.

Address correspondence to: Kristian Gundersen, Department of Molecular Biosciences, University of Oslo, PO Box 1041, Blindern, N-0316 Oslo, Norway. Phone: (47) 22-85-46-17; Fax: (47) 22-85-46-64; E-mail: kgunder@imbv.uio.no.

1. Gundersen, K. 1998. Determination of muscle contractile properties: The importance of the nerve. *Acta Physiol. Scand.* **162**:333–341.
2. Glass, D.J. 2003. Signalling pathways that mediate skeletal muscle hypertrophy and atrophy. *Nat. Cell Biol.* **5**:87–90.
3. Glass, D.J. 2005. Skeletal muscle hypertrophy and atrophy signaling pathways. *Int. J. Biochem. Cell Biol.* **37**:1974–1984.
4. Jackman, R.W., and Kandarian, S.C. 2004. The molecular basis of skeletal muscle atrophy. *Am. J. Physiol. Cell Physiol.* **287**:C834–C843.
5. Allen, D.L., et al. 1996. Myonuclear number and myosin heavy chain expression in rat soleus single muscle fibers after spaceflight. *J. Appl. Physiol.* **81**:145–151.
6. Allen, D.L., et al. 1997. Apoptosis: a mechanism contributing to remodeling of skeletal muscle in response to hindlimb unweighting. *Am. J. Physiol.* **273**:C579–C587.
7. Allen, D.L., et al. 1997. Growth hormone/IGF-I and/or resistive exercise maintains myonuclear number in hindlimb unweighted muscles. *J. Appl. Physiol.* **83**:1857–1861.
8. Alway, S.E., Martyn, J.K., Ouyang, J., Chaudhrai, A., and Murlasits, Z.S. 2003. Id2 expression during apoptosis and satellite cell activation in unloaded and loaded quail skeletal muscles. *Am. J. Physiol. Regul Integr Comp Physiol* **284**:R540–R549.
9. Alway, S.E., Degens, H., Krishnamurthy, G., and Chaudhrai, A. 2003. Denervation stimulates apoptosis but not Id2 expression in hindlimb muscles of aged rats. *J. Gerontol. A Biol. Sci. Med. Sci.* **58**:687–697.
10. Darr, K.C., and Schultz, E. 1989. Hindlimb suspension suppresses muscle growth and satellite cell proliferation. *J. Appl. Physiol.* **67**:1827–1834.
11. Dupont-Versteegden, E.E., Murphy, R.J.L., Houlè, J.D., Gurley, C.M., and Peterson, C.A. 1999. Activated satellite cells fail to restore myonuclear number in spinal cord transected and exercised rat. *Am. J. Physiol.* **277**:C589–C597.
12. Dupont-Versteegden, E.E., Murphy, R.J., Houle, J.D., Gurley, C.M., and Peterson, C.A. 2000. Mechanisms leading to restoration of muscle size with exercise and transplantation after spinal cord injury. *Am. J. Physiol. Cell Physiol.* **279**:C1677–C1684.
13. Gallegly, J.C., et al. 2004. Satellite cell regulation of muscle mass is altered at old age. *J. Appl. Physiol.* **97**:1082–1090.
14. Hikida, R.S., et al. 1997. Myonuclear loss in atrophied soleus muscle fibers. *Anat. Rec.* **247**:350–354.
15. Leeuwenburgh, C., Gurley, C.M., Strotman, B.A., and Dupont-Versteegden, E.E. 2005. Age-related differences in apoptosis with disuse atrophy in soleus muscle. *Am. J. Physiol. Regul. Integr. Comp. Physiol.* **288**:R1288–R1296.
16. Schmalbruch, H., and Lewis, D.M. 2000. Dynamics of nuclei of muscle fibers and connective tissue cells in normal and denervated rat muscles. *Muscle Nerve.* **23**:617–626.
17. Viguie, C.A., Lu, D.X., Huang, S.K., Rengen, H., and Carlson, B.M. 1997. Quantitative study of the effects of long-term denervation on the extensor digitorum longus muscle of the rat. *Anat. Rec.* **248**:346–354.
18. Adhihetty, P.J., O'Leary, M.F., Chabi, B., Wicks, K.L., and Hood, D.A. 2007. Effect of denervation on mitochondrially mediated apoptosis in skeletal muscle. *J. Appl. Physiol.* **102**:1143–1151.
19. Borisov, A.B., and Carlson, B.M. 2000. Cell death in denervated skeletal muscle is distinct from classical apoptosis. *Anat. Rec.* **258**:305–318.
20. Jin, H., Wu, Z., Tian, T., and Gu, Y. 2001. Apoptosis in atrophic skeletal muscle induced by brachial plexus injury in rats. *J. Trauma.* **50**:31–35.
21. Siu, P.M., and Alway, S.E. 2005. Mitochondria-associated apoptotic signalling in denervated rat skeletal muscle. *J. Physiol.* **565**:309–323.
22. Tang, H., Cheung, W.M., Ip, F.C., and Ip, N.Y. 2000. Identification and characterization of differentially expressed genes in denervated muscle. *Mol. Cell. Neurosci.* **16**:127–140.
23. Tews, D.S., et al. 1997. DNA-fragmentation and expression of apoptosis-related proteins in experimentally denervated and reinnervated rat facial muscle. *Neuropathol. Appl. Neurobiol.* **23**:141–149.
24. Yoshimura, K., and Harii, K. 1999. A regenerative change during muscle adaptation to denervation in rats. *J. Surg. Res.* **81**:139–146.
25. Dupont-Versteegden, E.E., et al. 2006. Nuclear translocation of EndoG at the initiation of disuse muscle atrophy and apoptosis is specific to myonuclei. *Am. J. Physiol. Regul. Integr. Comp. Physiol.* **291**:R1730–R1740.
26. Siu, P.M., Pistilli, E.E., and Alway, S.E. 2005. Apoptotic responses to hindlimb suspension in gastrocnemius muscles from young adult and aged rats. *Am. J. Physiol. Regul. Integr. Comp. Physiol.* **289**:R1015–R1026.
27. Siu, P.M., Pistilli, E.E., Butler, D.C., and Alway, S.E. 2005. Aging influences cellular and molecular responses of apoptosis to skeletal muscle unloading. *Am. J. Physiol. Cell Physiol.* **288**:C338–C349.
28. Tews, D.S. 2005. Muscle-fiber apoptosis in neuromuscular diseases. *Muscle Nerve.* **32**:443–458.
29. Utvik, J.K., Njå, A., and Gundersen, K. 1999. DNA injection into single cells of intact mice. *Hum. Gene Ther.* **10**:291–300.
30. Rana, Z.A., Gundersen, K., Buonanno, A., and Vullhorst, D. 2004. Imaging transcription in vivo: distinct regulatory effects of fast and slow activity patterns on promoter elements from troponin I isoform genes. *J. Physiol.* **562**:815–828.
31. Lichtman, J.W., Magrassi, L., and Purves, D. 1987. Visualization of neuromuscular junctions over periods of several months in living mice. *J. Neurosci.* **7**:1215–1222.
32. Wada, K.I., Takahashi, H., Katsuta, S., and Soya, H. 2002. No decrease in myonuclear number after long-term denervation in mature mice. *Am. J. Physiol. Cell Physiol.* **283**:C484–C488.
33. Brack, A.S., Bildsoe, H., and Hughes, S.M. 2005. Evidence that satellite cell decrement contributes to preferential decline in nuclear number from large fibres during murine age-related muscle atrophy. *J. Cell Sci.* **118**:4813–4821.
34. Schmalbruch, H., and Hellhammer, U. 1977. The number of nuclei in adult rat muscles with special reference to satellite cells. *Anat. Rec.* **189**:169–176.
35. Bruusgaard, J.C., Liestol, K., Ekmark, M., Kollstad, K., and Gundersen, K. 2003. Number and spatial distribution of nuclei in the muscle fibres of normal mice studied in vivo. *J. Physiol.* **551**:467–478.
36. Gundersen, K., and Mæhlen, J. 1994. Nerve-evoked electrical activity regulates molecules and cells with immunological function in rat muscle tissue. *Eur. J. Neurosci.* **6**:1113–1118.
37. Rosser, B.W., Dean, M.S., and Bandman, E. 2002. Myonuclear domain size varies along the lengths of maturing skeletal muscle fibers. *Int. J. Dev. Biol.* **46**:747–754.
38. Siu, P.M., Pistilli, E.E., Butler, D.C., and Alway, S.E. 2004. Aging influences the cellular and molecular responses of apoptosis to skeletal muscle unloading. *Am. J. Physiol. Cell Physiol.* **288**:C338–C349.
39. Gundersen, K., and Merlie, J.P. 1994. Id-1 as a possible transcriptional mediator of muscle disuse atrophy. *Proc. Natl. Acad. Sci. U. S. A.* **91**:3647–3651.
40. Strassburger, E. 1893. Über die Wirkungssphäre der kerne und die zellgrösse [In German]. *Histologische Beiträge.* **5**:97–124.
41. Allen, D.L., Roy, R.R., and Edgerton, V.R. 1999. Myonuclear domains in muscle adaptation and disease. *Muscle Nerve.* **22**:1350–1360.
42. Edgerton, V.R., Roy, R.R., Allen, D.L., and Monti, R.J. 2002. Adaptations in skeletal muscle disuse or decreased-use atrophy. *Am. J. Phys. Med. Rehabil.* **81**:S127–S147.
43. Dupont-Versteegden, E.E. 2006. Apoptosis in skeletal muscle and its relevance to atrophy. *World J. Gastroenterol.* **12**:7463–7466.
44. Bruusgaard, J.C., Liestol, K., and Gundersen, K. 2006. Distribution of myonuclei and microtubules in live muscle fibers of young, middle-aged, and old mice. *J. Appl. Physiol.* **100**:2024–2030.

45. Saraste, A., and Pulkki, K. 2000. Morphologic and biochemical hallmarks of apoptosis. *Cardiovasc. Res.* **45**:528–537.
46. Hennig, R., and Lømo, T. 1987. Effects of chronic stimulation on the size and speed of long-term denervated and innervated rat fast and slow skeletal muscles. *Acta Physiol. Scand.* **130**:115–131.
47. Kern, H., Salmons, S., Mayr, W., Rossini, K., and Carraro, U. 2004. Recovery of long-term denervated human muscles induced by electrical stimulation. *Muscle Nerve.* **31**:98–101.
48. Reid, B., Martinov, V.N., Nja, A., Lomo, T., and Bewick, G.S. 2003. Activity-dependent plasticity of transmitter release from nerve terminals in rat fast and slow muscles. *J. Neurosci.* **23**:9340–9348.
49. Martinov, V.N., and Nja, A. 2005. A microcapsule technique for long-term conduction block of the sciatic nerve by tetrodotoxin. *J Neurosci Methods.* **141**:199–205.
50. Ni, H., et al. 2000. Persistence of platelet thrombus formation in arterioles of mice lacking both von Willebrand factor and fibrinogen. *J. Clin. Invest.* **106**:385–392.
51. Rich, M.M., and Lichtman, J.W. 1989. In vivo visualization of pre- and postsynaptic changes during synapse elimination in reinnervated mouse muscle. *J. Neurosci.* **9**:1781–1805.